

Nanoscale superconductors: quantum confinement and spatially dependent Hartree-Fock potential

Yajiang Chen, M. D. Croitoru, A. A. Shanenko,^{*} and F. M. Peeters[†]

Departement Fysica, Universiteit Antwerpen, Groenenborgerlaan 171, B-2020 Antwerpen, Belgium

(Dated: November 3, 2018)

It is well-known that in bulk, the solution of the Bogoliubov-de Gennes equations is the same whether or not the Hartree-Fock term is included. In this case the Hartree-Fock potential is position independent and, so, gives the same contribution to both the single-electron energies and the Fermi level (the chemical potential). Thus, the single-electron energy measured from the Fermi level (it controls the solution) stays the same. It is not the case for nanostructured superconductors, where quantum confinement breaks the translational symmetry and results in a position dependent Hartree-Fock potential. Now the contribution of the Hartree-Fock mean field to the single-electron energies depends on the relevant quantum numbers. Moreover, the single-electron wave functions can be influenced by the presence of this additional spatially dependent field. We numerically solved the Bogoliubov-de Gennes equations with the Hartree-Fock term for a clean metallic nanocylinder and found a shift of the curve representing the thickness-dependent oscillations of the critical temperature (the energy gap, the order parameter etc.) to larger diameters. Though the difference between the superconducting solutions with and without the Hartree-Fock interaction can, for some diameters, be very significant, the above mentioned shift is less than typical metallic unit-cell dimensions and, so, has no practical worth. This allows one to significantly simplify the problem and, similar to bulk, ignore the Hartree-Fock potential when solving the Bogoliubov-de Gennes equations in the nano-regime.

PACS numbers: 74.78.-w, 74.78.Na

I. INTRODUCTION

Advances in nanofabrication technology resulted recently in high-quality metallic superconducting ultrathin nanofilms^{1,2,3} and nanowires.^{4,5,6,7} In most samples the electron mean free path was estimated to be about or larger than the nanofilm/nanowire thickness.^{2,4,7} In this case the effects of the transverse quantization are not shadowed by impurity scattering and, hence, the conduction band splits up into a series of single-electron subbands resulting from the quantized transverse modes. This will have a pronounced effect on the superconducting properties (see, for instance, Refs. 8 and 9 and references therein). Notice that high-quality nanofilms do not exhibit significant indications of defect- or phase-driven suppression of superconductivity (see discussion in Ref. 2). For high-quality nanowires the phase-fluctuation effects were shown to seriously influence the superconducting state only in narrowest aluminum specimens with width $\approx 5 - 8$ nm.^{4,7,10} Thus, the transverse quantum confinement is the major mechanism governing the superconducting properties in this case. Therefore, it is timely to study in a more detail a clean nanoscale superconductor in the presence of quantum confinement.

Quantum confinement breaks the translational symmetry and, so, the superconducting order parameter becomes position dependent. The well-known BCS ansatz for the ground state wave function is not applicable in this case, and the Bogoliubov-de Gennes (BdG) equations are a relevant tool to investigate equilibrium superconducting properties. Recent numerical studies of the BdG equations for nanofilms⁸ and nanowires^{9,11,12} show

that the transverse quantum confinement has a substantial impact on the superconducting solution. However, the BdG equations investigated in Refs. 8, 9, 11 and 12, were solved without the Hartree-Fock (HF) potential. The reason is that in bulk, the superconducting solution is not sensitive to the HF term in the BdG equations¹³, and one can assume that a similar conclusion holds for the broken translational symmetry. However, at present there is no detailed investigations on this subject and, so, such a study is needed.

In the bulk BdG equations, the HF potential is not spatially dependent and, so, it produces the same contribution to all single-electron energies, with no dependence on the relevant quantum numbers. Hence, the Fermi level (the chemical potential) acquires the same contribution, as well, and the single-electron energies measured from the Fermi level are not changed. It is well-known that the BdG equations are derived within the grand canonical formalism and, so, the electron energies appearing in the basic expressions absorb the chemical potential. As a result, the superconducting solution is insensitive to the HF potential. The situation is different in the presence of quantum confinement. The translational symmetry is now broken, the HF mean field is position dependent, and, so, its contribution to the single-electron energies is a function of the relevant quantum numbers. Furthermore, the single-electron wave functions themselves are influenced by the presence of the HF field, i.e., an additional spatially-dependent potential. Therefore, one can expect that the HF term in the BdG equations can change the superconducting solution in the presence of quantum confinement. It is of importance to clarify to what extent this will be through. In particular, this con-

cerns the thickness-dependent oscillations (i.e., quantum-size oscillations) of the superconducting properties typical of high-quality nanofilms and nanowires.^{1,2,8,9}

In the present work, based on the particular case of a superconducting clean metallic nanowire of the cylindrical form, we compare the superconducting numerical solutions of the BdG equations with and without the HF potential. We find that these solutions are indeed different and, for some nanocylinder diameters, this can be very significant. However, a more close look reveals that this difference is actually expressed in a small shift of the curve representing thickness-dependent oscillations of the critical temperature (or other important superconducting quantities) up to larger diameters. The shift is less than typical metallic unit-cell dimensions and, so, can be ignored.

The paper is organized as follows. In Sec. II the formalism of the BdG equations is outlined, with the focus on the features related to the cylindrical confining geometry. In addition, the Anderson approximate solution to the BdG equations is discussed in this section. To check the effect of the HF term on the single-electron wave functions, the Anderson solution is constructed by assuming that these wave functions do not change in the presence of the HF interaction. In Sec. III numerical results of the BdG equations with and without the HF term are discussed. Based on the Anderson solution, here we also investigate the effect of the HF term on the single-electron wave functions.

II. BOGOLIUBOV-DE GENNES EQUATIONS AND ANDERSON'S RECIPE

We focus on the basic superconducting properties of a metallic clean cylindrical nanowire (with diameter $D = 2R$ and length L) in the quantum-size regime when the transverse quantization of the single-electron spectrum is of importance. In the presence of quantum confinement the translational invariance is broken, and the order parameter appears to be position-dependent, i.e., $\Delta(\mathbf{r})$. It is well-known that the BdG equations are a common and useful approach to investigate such a situation. Generally, these equations can be represented as follows:

$$E_\nu |u_\nu\rangle = \hat{H}_e |u_\nu\rangle + \hat{\Delta} |v_\nu\rangle, \quad (1a)$$

$$E_\nu |v_\nu\rangle = \hat{\Delta}^* |u_\nu\rangle - \hat{H}_e^* |v_\nu\rangle, \quad (1b)$$

where E_ν stands for the quasiparticle energy, $|u_\nu\rangle$ and $|v_\nu\rangle$ are the particle-like and hole-like ket vectors. In the clean limit the single-electron Hamiltonian in Eqs. (1a) and (1b) is of the form [for zero magnetic field, $\mathbf{A} = 0$]

$$\hat{H}_e = \hat{H}_e^* = \frac{\hat{\mathbf{p}}^2}{2m_e} + \Phi_{HF}(\hat{\mathbf{r}}) + V_{\text{conf}}(\hat{\mathbf{r}}) - E_F, \quad (2)$$

with $\hat{\mathbf{r}}$ and $\hat{\mathbf{p}}$ the position and momentum operators, E_F the Fermi level, m_e the electron band mass (set to the free electron mass), $V_{\text{conf}}(\mathbf{r})$ the confining interaction, and

$\Phi_{HF}(\mathbf{r})$ the HF potential. In bulk the confining interaction can be neglected and we arrive at the usual BCS picture based on plane waves. Below we adopt the simplest choice of the confining interaction potential: zero inside and infinite outside the wire. The gap-operator $\hat{\Delta}$ in Eqs. (1a) and (1b) is related to the order parameter by $\hat{\Delta} = \Delta(\hat{\mathbf{r}})$.

As a mean-field theory, the BdG equations are solved in a self-consistent manner with the self-consistency relations given by

$$\Delta(\mathbf{r}) = g \sum_{\nu \in \mathcal{C}} \langle \mathbf{r} | u_\nu \rangle \langle v_\nu | \mathbf{r} \rangle [1 - 2f_\nu], \quad (3a)$$

$$\Phi_{HF}(\mathbf{r}) = -g \sum_{\nu} \left[|\langle \mathbf{r} | u_\nu \rangle|^2 f_\nu + |\langle \mathbf{r} | v_\nu \rangle|^2 (1 - f_\nu) \right], \quad (3b)$$

where $g > 0$ is the coupling constant, $f_\nu = 1/(e^{\beta E_\nu} + 1)$ is the Fermi function [$\beta = 1/(k_B T)$ with T the temperature and k_B the Boltzmann constant]. In Eq. (3a) \mathcal{C} indicates the set of quantum numbers corresponding to the single-electron energy ξ_ν (measured from the Fermi level) located in the Debye window $\xi_{\nu \in \mathcal{C}} \in [-\hbar\omega_D, \hbar\omega_D]$ (ω_D is the Debye frequency), where ξ_ν absorbs the HF potential, i.e.,

$$\xi_\nu = \langle u_\nu | \hat{H}_e | u_\nu \rangle + \langle v_\nu | \hat{H}_e^* | v_\nu \rangle. \quad (4)$$

The cut-off in Eq. (3a) is known¹⁴ to be a payment for using a simplified delta-function approximation for the electron-electron interaction. Such a regularization is not needed in Eq. (3b). For our confining interaction (i.e., zero inside and infinite outside) we have

$$\langle \mathbf{r} | u_\nu \rangle \Big|_{\mathbf{r} \in S} = \langle \mathbf{r} | v_\nu \rangle \Big|_{\mathbf{r} \in S} = 0 \quad (5)$$

at the sample surface, i.e., $\mathbf{r} \in S$. Periodic boundary conditions with unit cell L can be applied in the direction parallel to the nanowire.

The Fermi level (i.e., the chemical potential) is determined from

$$n_e = \frac{2}{\pi R^2 L} \sum_{\nu} \left[\langle u_\nu | u_\nu \rangle f_\nu + \langle v_\nu | v_\nu \rangle (1 - f_\nu) \right], \quad (6)$$

where n_e is the mean electron density. We use the BdG equations in the parabolic band approximation and, so, as discussed in Ref. 8, an effective Fermi level should be introduced, to recover the correct period of the quantum-size oscillations. For aluminum (the aluminum parameters are used below) $E_F = 0.9 \text{ eV}$ for $D \approx 10 \text{ nm}$ (see Ref. 9). For $D \sim 1 - 2 \text{ nm}$, E_F shifts systematically from this value up, due to Eq. (6).

Due to the chosen confining geometry, it is convenient to use cylindrical coordinates ρ, φ and z . In this case the order parameter (the anomalous pairing potential) and HF mean field (the normal potential) depend only on the transverse coordinate, i.e., $\Delta(\rho)$ and $\Phi_{HF}(\rho)$, and $\langle \mathbf{r} | u_\nu \rangle$ and $\langle \mathbf{r} | v_\nu \rangle$ are represented in the form ($\nu = \{j, m, k\}$)

$$\begin{pmatrix} \langle \mathbf{r} | u_{jmk} \rangle \\ \langle \mathbf{r} | v_{jmk} \rangle \end{pmatrix} = \frac{e^{im\varphi} e^{ikz}}{\sqrt{2\pi} \sqrt{L}} \begin{pmatrix} u_{jmk}(\rho) \\ v_{jmk}(\rho) \end{pmatrix}, \quad (7)$$

with j controlling the number of nodes in the transverse direction, m the azimuthal quantum number, and k the wave vector of the quasi-free electron motion along the nanocylinder. Inserting Eq. (7) into Eqs. (1a) and (1b), we recast the BdG equations as

$$[E_{jmk} - \mathcal{L}_\rho - \Phi_{HF}(\rho)] u_{jmk}(\rho) = \Delta(\rho) v_{jmk}(\rho), \quad (8a)$$

$$[E_{jmk} + \mathcal{L}_\rho + \Phi_{HF}(\rho)] v_{jmk}(\rho) = \Delta(\rho) u_{jmk}(\rho), \quad (8b)$$

where $\Delta(\rho)$ is real, and

$$\mathcal{L}_\rho = -\frac{\hbar^2}{2m_e} \left(\frac{\partial^2}{\partial \rho^2} + \frac{1}{\rho} \frac{\partial}{\partial \rho} - \frac{m^2}{\rho^2} - k^2 \right) - E_F. \quad (9)$$

The self-consistency relations can be rewritten as,

$$\Delta(\rho) = \frac{g}{2\pi L} \sum_{jmk \in C} u_{jmk}(\rho) v_{jmk}(\rho) [1 - 2f_{jmk}], \quad (10a)$$

$$\Phi_{HF}(\rho) = -\frac{g}{2\pi L} \sum_{jmk} \left[u_{jmk}^2(\rho) f_{jmk} + v_{jmk}^2(\rho) (1 - f_{jmk}) \right], \quad (10b)$$

with $u_{jmk}(\rho)$ and $v_{jmk}(\rho)$ real. To numerically solve Eqs. (8a) and (8b), we expand the transverse particle-like and hole-like wave functions as

$$\begin{pmatrix} u_{jmk}(\rho) \\ v_{jmk}(\rho) \end{pmatrix} = \sum_J \begin{pmatrix} u_{jmk,J} \\ v_{jmk,J} \end{pmatrix} \vartheta_{Jm}(\rho), \quad (11)$$

with

$$\vartheta_{Jm}(\rho) = \frac{\sqrt{2}}{R \mathcal{J}_{m+1}(\alpha_{Jm})} \mathcal{J}_m(\alpha_{Jm} \frac{\rho}{R}), \quad (12)$$

where $\mathcal{J}_m(x)$ is the Bessel function of the first kind of the m -order, and α_{Jm} is the J th zero of this function. This allows one to convert Eqs. (8a) and (8b) into a matrix form. Then, a numerical solution can be obtained by diagonalizing the corresponding matrix, and self-consistency is reached by iterating Eqs. (10a) and (10b). One should keep in mind that¹⁴ $\langle u_\nu | u_\nu \rangle + \langle v_\nu | v_\nu \rangle = 1$ and, so,

$$\int_0^R d\rho \rho [u_{jmk}^2(\rho) + v_{jmk}^2(\rho)] = 1. \quad (13)$$

As seen, the vector $(u_{jmk,J}; v_{jmk,J})^T$ ($J = 0, 1, \dots$) is normalized.

In addition to the above procedure, below we use the Anderson approximate solution, as well¹⁵. Within this approximation, instead of the expansion given by Eq. (11), it is assumed that

$$u_{jmk}(\rho) = \mathcal{U}_{jmk} \vartheta_{jm}(\rho), \quad v_{jmk}(\rho) = \mathcal{V}_{jmk} \vartheta_{jm}(\rho). \quad (14)$$

Equation (14) means that we seek a minimum of the BdG thermodynamic functional in the subspace of $u_{jmk}(\rho)$ and $v_{jmk}(\rho)$ proportional to the eigenfunctions of \mathcal{L}_ρ .

Notice that it is possible to deal with Anderson's recipe, invoking the eigenfunctions of $\mathcal{L}_\rho + \Phi_{HF}(\rho)$. However, below we are interested in Eq. (14) because it helps to clarify how a change in the single-electron wave functions due to the HF potential, can contribute to the problem of interest. To be accurate, the Anderson approximation should be based on the true single-electron wave functions. We recently found that in this case the error in Anderson's solution for $D \lesssim 2 - 3$ nm is less than one-two percents.¹⁶ Hence, comparing the results of numerically solving Eqs. (8a) and (8b) with the data based on Eq. (14), we can reach unambiguous conclusions about the role of the changes in the single-electron wave functions due to the HF interaction. As follows from Eq. (14) [see, for instance, Ref. 16], the Anderson-approximation results in the BCS-like self-consistent equation

$$\Delta_{j'm'} = -\frac{1}{2} \sum_{jmk \in C} \frac{g_{j'm',jm} \Delta_{jm}}{\sqrt{\xi_{jmk}^2 + \Delta_{jm}^2}} [1 - 2f_{jmk}], \quad (15)$$

with

$$\Delta_{jm} = \int_0^R d\rho \rho \vartheta_{jm}^2(\rho) \Delta(\rho) \quad (16)$$

and the interaction-matrix element given by

$$g_{j'm',jm} = -\frac{g}{2\pi L} \int_0^R d\rho \rho \vartheta_{j'm'}^2(\rho) \vartheta_{jm}^2(\rho). \quad (17)$$

For the single-electron energy appearing in Eq. (15) we have

$$\xi_{jmk} = \frac{\hbar^2}{2m_e} \left[\frac{\alpha_{jm}^2}{R^2} + k^2 \right] + \Phi_{jm} - E_F, \quad (18)$$

where

$$\Phi_{jm} = \int_0^R d\rho \rho \vartheta_{jm}^2(\rho) \Phi_{HF}(\rho). \quad (19)$$

Inserting Eq. (3b) into Eq. (19), one obtains

$$\Phi_{j'm'} = \frac{1}{2} \sum_{jmk} g_{j'm',jm} \left[1 - \frac{\xi_{jmk}(1 - 2f_{jmk})}{\sqrt{\xi_{jmk}^2 + \Delta_{jm}^2}} \right]. \quad (20)$$

We should not forget about E_F appearing in the single-electron energy given by Eq. (18). It is fixed through Eq. (6) that is now of the form

$$n_e = \frac{1}{\pi R^2 L} \sum_{jmk} \left[1 - \frac{\xi_{jmk}(1 - 2f_{jmk})}{\sqrt{\xi_{jmk}^2 + \Delta_{jm}^2}} \right]. \quad (21)$$

Thus, in the Anderson approximation introduced by Eq. (14), one needs to solve Eqs. (15) and (20), keeping Eq. (21). As already mentioned above, comparing a numerical solution of Eqs. (8a) and (8b) with the solution based on Anderson's recipe, we can check the effect of the HF interaction on the single-electron wave functions.

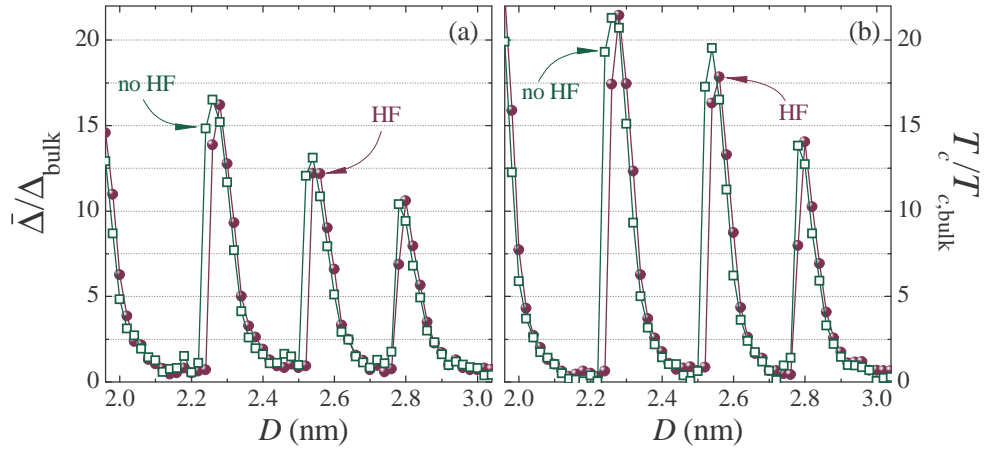


FIG. 1: (a) The spatially averaged superconducting order parameter $\bar{\Delta}/\Delta_{\text{bulk}}$ and (b) critical temperature $T_c/T_{c,\text{bulk}}$ versus the nanowires diameter D as calculated from the BdG equations (8a) and (8b) at zero temperature.

III. NUMERICAL RESULTS

In this section we investigate and discuss numerical self-consistent solutions of Eqs. (8a) and (8b) with the HF potential (the full version) and without it (the truncated version, by setting $\Phi_{HF}(\rho) = 0$ in the relevant expressions). Results are also compared with a solution of Eqs. (15) and (20). All the calculations are performed with the parameters typical for aluminum^{13,14}: $\hbar\omega_D = 32.31$ meV; $gN(0) = 0.18$, with $N(0) = m_e k_F / (2\pi^2 \hbar^2)$ the bulk density of single-electron states at the Fermi level [for E_F see discussion after Eq. (6)] and k_F the bulk Fermi wavevector. For these parameters the bulk BCS coherence length $\xi_0 = 1.6$ μm is significantly larger than the nanocylinder diameter. However, contrary to the ordinary Ginzburg-Landau picture, the superconducting order parameter now exhibits significant spatial variations in the transverse direction due to the broken translational symmetry. The length of the nanocylinder is taken as $L = 1$ $\mu\text{m} \gg \lambda_F = 2\pi/k_F$. This is an optimal choice, upholding, on one side, the use of periodic boundary conditions in the z direction and, on the other side, it results in a reasonable calculational time. As opposed to the truncated BdG equations, their full version requires much more time for convergence of the numerical procedure, and this time increases proportionally with L^2 . Numerically solving the Anderson equations (15) and (20) is less time-consuming and, so, we take $L = 5$ μm in this case.

In Fig. 1(a) the spatially averaged order parameter

$$\bar{\Delta} = \frac{2}{R^2} \int_0^R d\rho \rho \Delta(\rho),$$

calculated from Eqs. (8a) and (8b), is plotted in units of the bulk order parameter ($\Delta_{\text{bulk}} = 0.25$ meV) versus the nanocylinder diameter with and without the HF mean field. In Fig. 1(b) the corresponding critical tempera-

ture T_c (in units of the bulk one) is given. As seen, both data-sets exhibit pronounced size-dependent oscillations, typical of high-quality superconducting nanofilms and nanowires with uniform thickness^{1,2,8,9}. Such oscillations result from single-electron subbands forming due to the transverse quantization of the electron motion. With an increase in the nanowire diameter, the subbands shift down in energy. Each time when a new subband comes into the Debye window around the Fermi level, the number of single-electron states contributing to the superconducting order parameter increases, and a size-dependent superconducting resonance develops. As follows from Fig. 1, the quantum-size oscillations corresponding to the full version of the BdG equations are somewhat shifted up. Hence, the difference between the two sets of data is most significant for those diameters, where a size-dependent superconducting resonance in the case without the HF interaction is already present while in the full version such a resonance only starts to develop. The difference is not so significant but still survive when the resonance comes into its decay stage. When the resonance is fully decayed (the off-resonant regime), the HF corrections are practically negligible, and we arrive at the situation similar to bulk. Notice that small differences between the numerical results of the full and truncated BdG equations in the off-resonant regime (due to beating patterns of the corresponding curves), are because of the chosen nanowire length. Indeed, as follows from calculations for several selected off-resonant diameters, such beating patterns disappear when L increases up to 20 – 30 μm , and the results with and without the HF interaction approach each other.

Notice that maxima of $T_c/T_{c,\text{bulk}}$ in Fig. 1(b) are generally higher than those of $\bar{\Delta}/\Delta_{\text{bulk}}$ in Fig. 1(a). This is due to formation of new Andreev-type states induced by the transverse quantum confinement (see details in Ref. 17), which results in a decrease of $\bar{\Delta}/(k_B T_c)$ below the bulk value 1.763 at the resonant points. As seen from

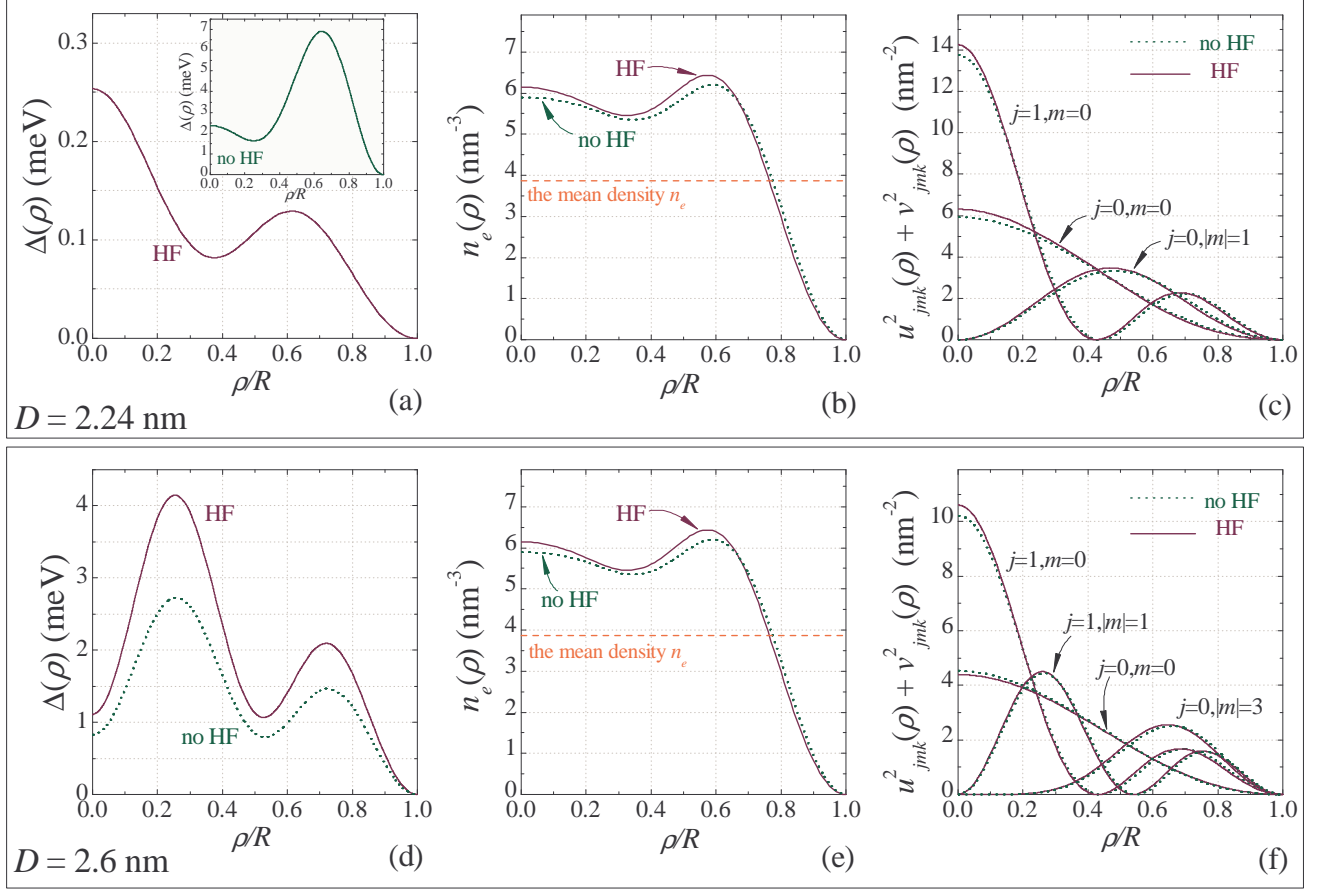


FIG. 2: Upper panel: (a) the superconducting order parameter $\Delta(\rho)$, (b) the local density $n_e(\rho)$ and (c) the distribution $u_{jmk}^2(\rho) + v_{jmk}^2(\rho)$ versus ρ/R for $D = 2.24$ nm. The lower panel: the same but for $D = 2.6$ nm. The results for the truncated (no HF) and full (HF) BdG equations are plotted.

Fig. 1, inclusion of the HF interaction can slightly reduce the resonant enhancements, with practically no effect on the ratio $\bar{\Delta}/(k_B T_c)$.

In Fig. 2 we present different quantities calculated with the full and truncated versions of Eqs. (8a) and (8b) for two diameters: the upper panel, for $D = 2.24$ nm; and the lower panel, for $D = 2.6$ nm. The upper panel represents the situation when a superconducting resonance is developed for the truncated version but is not yet present for the full version of the BdG equations. In Fig. 2(a) the superconducting order parameter $\Delta(\rho)$ calculated with (HF) and without the HF interaction (no HF, the inset), is plotted versus the transverse coordinate ρ/R for $T = 0$. The spatial distribution of the pair condensate is very different for these two cases: the data without the HF interaction are larger by an order of magnitude, and even the profile of $\Delta(\rho)$ is different. In Fig. (2)(b) the local electron density, i.e.,

$$n_e(\rho) = \frac{1}{\pi L} \sum_{jmk} \left[u_{jmk}^2(\rho) f_{jmk} + v_{jmk}^2(\rho) (1 - f_{jmk}) \right], \quad (22)$$

is shown for the same diameter. As can be expected,

now the difference between the two data-sets is not so significant (we keep to the same value of the mean electron density n_e). Due to the attractive character of the effective electron-electron interaction, the HF potential forces electrons to go closer to the nanocylinder center. However, the confining interaction has the major effect on $n_e(\rho)$ as compared to the HF potential producing only some small corrections. From the results for the local electron density, it is possible to expect that the single-electron wave functions are also not very sensitive to the HF interaction. For nanowires, $|u_\nu(\mathbf{r})|$ and $|v_\nu(\mathbf{r})|$ is nearly proportional to the corresponding single-electron wave function [see discussion above, after Eq. (14)]. Hence, due to Eq. (13), the quantity $u_{jmk}^2(\rho) + v_{jmk}^2(\rho)$ can provide us with the information about the single-electron distribution. In Fig. 2(c) $u_{jmk}^2(\rho) + v_{jmk}^2(\rho)$ is plotted versus ρ/R for the quantum numbers most sensitive to including the HF interaction. We can indeed see that the effect of the HF potential on the wave functions is minor. Similar conclusions can be obtained from the lower panel of Fig. 2. The only exception is that the superconducting order parameter in Fig. 2(d) [$D = 2.6$ nm] does not change so much when

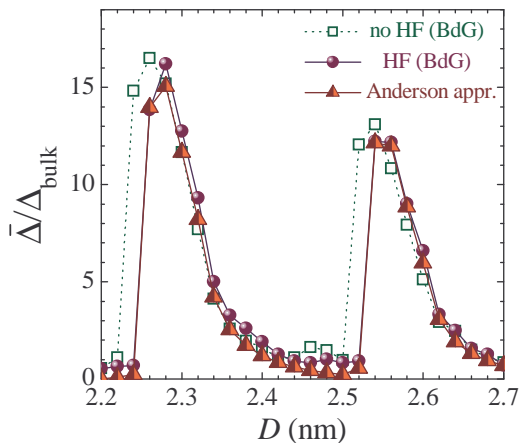


FIG. 3: $\bar{\Delta}/\Delta_{\text{bulk}}$ versus the nanowire diameter ($T = 0$): triangles correspond to the Anderson approximation [the HF field is included]; stars and squares are the numerical results of the full and truncated BdG equations, respectively.

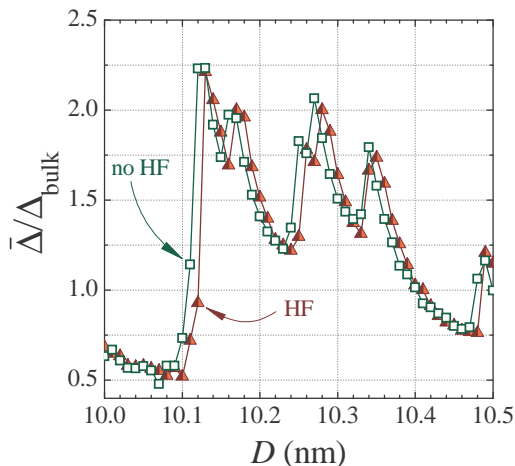


FIG. 4: HF versus no HF: $\bar{\Delta}/\Delta_{\text{bulk}}$ as a function of the nanowire diameter D at zero temperature [squares are the results of the truncated BdG equations (no HF interaction); triangles are the results of the Anderson approximation, see Eqs. (15) and (19)].

including the HF potential. Notice that $n_e(\rho)$ given in Fig. 2(e) is practically the same as in Fig. 2(b). However, this is not true for $u_{jmk}^2(\rho) + v_{jmk}^2(\rho)$ [compare panel (c) with panel (f)]. The point is that the integral $\int_0^R d\rho \rho n_e(\rho) = n_e R^2/2$ changes with the radius but for the single-electron distribution $u_{jmk}^2(\rho) + v_{jmk}^2(\rho)$ we have Eq. (13)].

From the results presented in Fig. 2, one expects minor effects on the single-electron wave functions due to the incorporation of the HF interaction. This expectation can be put on a more solid ground by using the Anderson approximation based on Eqs. (15) and (19). We remind that the Anderson approximation is quite good for superconducting nanowires provided that it involves

the true single-electron wave functions. Equations (15) and (19) follow from Eq. (14) and, hence, as assumed, the single-electron wave functions are not altered by our position-dependent HF interaction. If this is a reasonable assumption, results of the Anderson approximation constructed in this way, should be close to the results of the full BdG equations. As seen from Fig. 3, this is indeed the case. We can conclude that the thickness-dependent shift of the superconducting resonances in the presence of the HF interaction has nothing to do with the single-electron wave functions. Its mechanism is due to the fact that the position-dependent HF potential results in a change of the single-electron energies measured from the Fermi level.

So far we considered extremely narrow nanowires, for the sake of simplicity. However, a similar shift ($\approx 0.01 - 0.02$ nm) of the quantum-size oscillations due to the HF term survives until the total decay of the quantum-size oscillations (up to diameters of about 50 – 70 nm). In particular, such a shift is clearly seen in Fig. 4, where numerical results of the truncated BdG equations for $D = 10 - 10.5$ nm are compared with a solution of Eqs. (15) and (19) including the HF potential. Thus, we arrive at the following picture. In the vicinity of a superconducting resonance, the bottom of some single-electron subband is situated close to the Fermi level. Therefore, a repositioning of this subband with respect to the Fermi level can result in a significant change of the number of single-electron states in the Debye window and, so, in a remarkable increase/decrease of superconducting characteristics. However, when bottoms of all single-electron subbands are quite apart from the Fermi level, i.e., in the off-resonant regime, a move of these subbands in energy produces much less important effect on the number of single-electron states located in the Debye window. This is why the decay of a superconducting resonance is accompanied by a depletion of the influence of the HF potential.

IV. CONCLUSIONS

Quantum confinement breaks the translational symmetry in nanostructured superconductors. In this case, despite the delta-function approximation for the electron-electron interaction, the HF potential becomes position dependent, and its contribution to the single-electron energy (measured from the Fermi level) is a function of the relevant quantum numbers (contrary to bulk!). By numerically solving the Bogoliubov-de Gennes equations for a clean metallic nanocylinder, we have shown that such a feature results in a shift of the curve representing the thickness-dependent oscillations of the critical temperature (the energy gap, the order parameter etc.) to larger diameters. Though difference between the numerical results with and without the HF potential can be rather significant for some given diameters, the above mentioned shift is less than typical metallic unit-cell dimensions and,

so, can be ignored. In particular, smoothing due to the thickness fluctuations in real samples will shadow this effect. Thus, when solving the Bogoliubov-de Gennes equations in the nano-regime, one is able to neglect the HF term, which significantly simplifies a numerical procedure.

Acknowledgments

Yajiang Chen thanks B. Xu and R. Geurt for helpful discussions. This work was supported by the Flemish Sci-

ence Foundation (FWO-VI), the Belgian Science Policy (IAP) and ESF-AQDJJ network.

* Electronic address: arkady.shanenko@ua.ac.be

† Electronic address: francois.peeters@ua.ac.be

¹ Y. Guo, Y.-F. Zhang, X.-Y. Bao, T.-Z. Han, Z. Tang, L.-X. Zhang, W.-G. Zhu, E.G. Wang, Q. Niu, Z. Q. Qiu, J.-F. Jia, Z.-X. Zhao, and Q. K. Xue, *Science* **306**, 1915 (2004).

² M. M. Özer, J. R. Thompson, and H. H. Weitering, *Nature Physics* **2**, 173 (2006); *ibid.*, *Phys. Rev. B* **74**, 235427 (2006); M. M. Özer, Y. Jia, Z. Zhang, J. R. Thompson, and H. H. Weitering, *Science* **316**, 1594 (2007).

³ D. Eom, S. Qin, M.-Y. Chou, and C. K. Shih, *Phys. Rev. Lett.* **96**, 027005 (2006).

⁴ M. Savolainen, V. Touboltsev, P. Koppinen, K.-P. Riikonen, and K. Arutyunov, *Appl. Phys. A*, **79**, 1769 (2004); M. Zgirski, K.-P. Riikonen, V. Touboltsev, V., and K. Arutyunov, *Nano Lett.* **5**, 1029 (2005); M. Zgirski, K. P. Riikonen, V. Touboltsev, P. P. Jalkanen, T. T. Hongisto, K. Y. Arutyunov, *Nanotechnology* **19**, 055301 (2008).

⁵ M. L. Tian, J. G. Wang, J. S. Kurtz, Y. Liu, M. H. W. Chan, T. S. Mayer, and T. E. Mallouk, *Phys. Rev. B* **71**, 104521 (2005).

⁶ L. Jankovič, D. Gournis, P. N. Trikalitis, I. Arfaoui, T. Cren, P. Rudolf, M.-H. Sage, T. T. M. Palstra, B. Kooi, J. De Hosson, M. A. Karakassides, K. Dimos, A. Moukarika, and T. Bakas, *Nano Lett.* **6**, 1131 (2006); N. Tombros, L. Buit, I. Arfaoui, T. Tsoufis, D. Gournis, P. N. Trikalitis, S. J. van der Molen, P. Rudolf, and B. J. van Wees, *Nano Lett.* **8**, 3060 (2008).

⁷ F. Altomare, A. M. Chang, M. R. Melloch, Y. Hong, and C. W. Tu, *Phys. Rev. Lett.* **97**, 017001 (2006).

⁸ A. A. Shanenko, M. D. Croitoru, and F. M. Peeters, *Europhys. Lett.* **76**, 498 (2006); *ibid.*, *Phys. Rev. B* **75**, 014519 (2007).

⁹ A. A. Shanenko and M. D. Croitoru, *Phys. Rev. B* **73**, 012510 (2006); A. A. Shanenko, M. D. Croitoru, M. Zgirski, F. M. Peeters, and K. Arutyunov, *Phys. Rev. B* **74**, 052502 (2006).

¹⁰ K. Yu. Arutyunov, D. S. Golubev, and A. D. Zaikin, *Phys. Rep.* **464**, 1 (2008).

¹¹ J. E. Han and V. H. Crespi, *Phys. Rev. B* **69**, 214526 (2004).

¹² I. Grigorenko, J.-X. Zhu, and A. Balatsky, *J. Phys.: Condens. Matter* **20**, 195204 (2008).

¹³ A. L. Fetter and J. D. Walecka, *Quantum Theory of Many-Particle Systems* (Dover, New York, 2003).

¹⁴ P. G. de Gennes, *Superconductivity of Metals and Alloys* (W. A. Benjamin, New York, 1966).

¹⁵ P. W. Anderson, *J. Phys. Chem. Solids* **11**, 26 (1959).

¹⁶ A. A. Shanenko, M. D. Croitoru, and F. M. Peeters, *Phys. Rev. B* **78**, 024505 (2008); *ibid.*, *Phys. Rev. B* **78**, 054505 (2008).

¹⁷ A. A. Shanenko, M. D. Croitoru, R. G. Mints, and F. M. Peeters, *Phys. Rev. Lett.* **99**, 067007 (2007).